

# Origin of compaction bands: Anti-cracking or constitutive instability?

Alexandre I. Chemenda\*

Géoazur, Université de Nice-Sophia Antipolis, CNRS, 250 Rue Albert Einstein, 06560 Valbonne, France

## ARTICLE INFO

### Article history:

Received 21 September 2009  
 Received in revised form 30 December 2010  
 Accepted 4 January 2011  
 Available online 13 January 2011

### Keywords:

Deformation localization  
 Compaction bands  
 Stability and bifurcation  
 Rock mechanics  
 Granular material  
 Finite-difference

## ABSTRACT

Based on the theoretical analysis and finite-difference simulations, we study the onset and evolution of tabular compaction bands. In numerical models the bands are initiated as constitutive instabilities resulting from the deformation bifurcation. Then some bands are dying, while others continue to evolve accumulating the inelastic deformation/damage and compressive stress at their tips. The stress concentration/increase, however, does not exceed 0.1% of the background value. Starting from some stage, the bands begin to propagate similarly to cracks. At the next stage the propagation slows down simultaneously with the beginning of bands' thickening that occurs due to incorporation of not yet compacted material at the band flanks. The response of the already compacted "core" part of the band becomes mostly elastic. Then the propagation practically stops and the bands undergo only the heterogeneous thickening, maximal in the middle of the band and reducing toward its tips. This scenario obtained directly in the models (without any specific hypotheses about the propagation mechanism) appears more complicated than what can be expected from the linear elastic fracture mechanics (anti-crack) model. The band propagation distance is proportional to the initial (resulted from the bifurcation) band length that in turn is proportional to the hardening modulus and theoretically can reach infinity.

© 2011 Elsevier B.V. All rights reserved.

## 1. Introduction

After the discovery of compaction bands in the field (Mollema and Antonellini, 1996), there has been a growing amount of studies of these features based on the theoretical analysis (e.g., Chemenda, 2009; Garagash, 2006; Issen, 2002; Issen and Rudnicki, 2000; Rudnicki, 2007; Sternlof et al., 2005; Tembe et al., 2008), the lattice (Katsman et al., 2005), discrete element (Wang et al., 2008), and finite-difference (Chemenda, 2009; Stefanov and Thiercelin, 2007) numerical modeling, as well as the experimental rock (e.g., Baud et al., 2004; Fortin et al., 2006; Olsson and Holcomb, 2000; Wong et al., 1997) and synthetic rock analogue (Nguyen et al., 2011) testing. It follows in particular that the aspect of compaction bands generated in the conventional axisymmetric compression tests in the cylindrical samples is not the same as that of the natural compaction bands. In the laboratory, these features typically represent tight zigzag discrete bands with fairly sharp angular junctions of the segments (Fig. 1a). They first appear at the sample along-axis ends and then progressively toward the sample middle, yielding a picture of a propagating (in the direction perpendicular to the bands) discrete banding. In the field, the compaction bands can have wavy (crooked) forms (Mollema and Antonellini, 1996) resembling the "experimental" bands, but they can also be linear (planar) and organized in regular tabular sets. The size

of the bands (their thickness  $d$  and length  $L$ ) can vary in large limits. For example, in the Jurassic Navajo Sandstone (Utah)  $d$  is 0.5–1.5 cm and  $L$ , 5–10 m (Mollema and Antonellini, 1996). In the Jurassic Aztec Sandstone (Valley of Fire, Nevada), Fig. 2 the bands are tens of meters long, 1–2 cm thick (in the middle), with band spacing  $\lambda$  of tens of centimeters (Sternlof et al., 2005).

The difference between the compaction bands generated in the laboratory and nature may suggest that the mechanism of their formation is also different. The "experimental" bands are often considered as resulting from the deformation bifurcation that leads to the formation of  $\sigma_1$ -orthogonal bands ( $\sigma_1 > \sigma_2 > \sigma_3$  are the principal stresses, the compressive stress is positive) (Issen and Rudnicki, 2000). This banding/localization regime was predicted theoretically in the frame of the continuous deformation bifurcation analysis (Issen and Rudnicki, 2000; Ottosen and Runesson, 1991; Perrin and Leblond, 1993) that considers the conditions of a constitutive instability in the case when the material within and outside the band is in the same elastic-plastic state. It was stated by different authors that conclusions of this analysis are in a quantitative disagreement with the available experimental data (e.g., Baud et al., 2006). In particular, the theory predicts a too negative value of the dilatancy factor  $\beta$  for the compaction banding to occur. Yet, it does not predict (consider) the propagating character of compaction banding and zigzag shape of the bands.

Based on the virtual work principle, Garagash (1981, 2006) considered a bifurcation resulting in a set of parallel loading bands with the material outside them undergoing elastic unloading.

\* Tel.: +33 4 9294 2661; fax: +33 4 9294 2610.  
 E-mail address: [chem@geoazur.unice.fr](mailto:chem@geoazur.unice.fr).

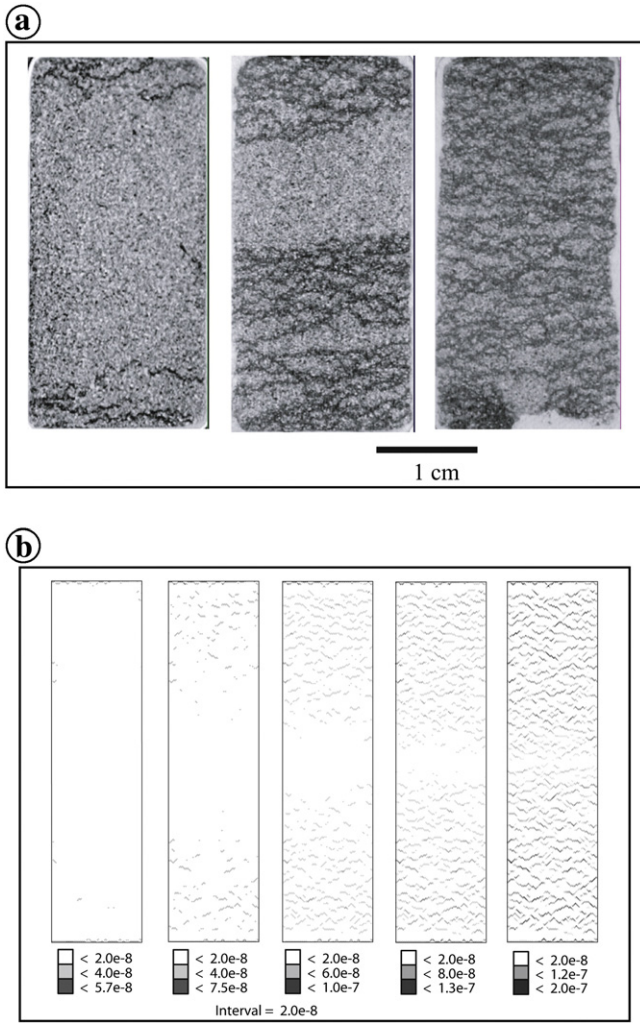


**Fig. 1.** (a) Discrete compaction banding in Bentheim sandstone sample under vertical axisymmetric compression at different axial strains (from Baud et al., 2004); (b) Patterns of accumulated inelastic equivalent shear deformation  $\bar{\gamma}^p$  for successive stages of the evolution of numerical model under axisymmetric compression stress (from Chemenda, 2009).

Chemenda (2009) analyzed this case (corresponding to the discontinuous bifurcation) using both classical bifurcation and finite-difference numerical approaches. Tight compaction bands were predicted at small negative  $\beta$  well corresponding to the experimentally obtained values. The numerical simulations confirmed this theoretical result and reproduced both zigzag shape of the bands and their progressive appearance from the sample (numerical model) ends (where the compressive load is applied) toward the middle (Fig. 1b). Such a propagation of the deformation in the direction perpendicular to the bands is caused by the boundary effect and is related to the evolution of the material constitute properties with deformation (Chemenda, 2009). Thus a constitutive instability seems to be rather a plausible mechanism of compaction banding observed in the laboratory experiments.

As far as long linear (planar) natural compaction bands are concerned, their thickness reduces from the central bands' segments toward the extremities (tips), Fig. 2b (Mollema and Antonellini, 1996; Sternlof et al., 2005). This suggests their penny-shape geometry in 3-D and compression anti-crack (opposed to tension mode I crack) propagation mechanism analyzed in the framework of linear elastic fracture mechanics (LEFM) (Fletcher and Pollard, 1981; Mollema and Antonellini, 1996; Rudnicki, 2007; Sternlof et al., 2005; Tembe et al., 2008). Such a mechanism is different from the deformation

bifurcation. It implies existence of soft/weak initiation zones (inclusions) where the band propagation can be initiated due to the stress concentration at the inclusions extremities.

In this paper we present results from the finite-difference simulations that reproduce tabular compaction bands. They are initiated as constitutive instabilities, then propagated similar to cracks along their strike and thickened during further deformation. As in the natural bands the thickness of “numerical” bands progressively reduces toward the band ends. The evolution of a tabular band set thus includes two mechanisms. The first one is the deformation bifurcation that results in the initiation of a set of bands that propagate at the next stage. This propagation resembles the propagation of an anti-crack. The stress concentration at the band tips is, however, very small and the propagation limited. At the initial stages of propagation the band thickness does not change and the material within the whole band (not only at its tips) is affected by the inelastic deformation (damage). At the later stages the band thickens and the inelastic deformation is concentrated along the band perimeter, while the response of the already compacted “core” part of the band becomes mostly elastic.

## 2. Summary of the results of multi-band discontinuous bifurcation analysis

The initiation of a compaction band set is supposed to occur through the constitutive instability, which defines the principal geometrical attributes of the set such as initial band spacing  $\lambda_0$ , length  $L_0$  and thickness  $d_0$ . These parameters will evolve during the post bifurcation deformation, but their final values will be strongly affected by the initial ones that can be predicted from the discontinuous bifurcation analysis. The complete analysis and all relevant references are given in (Chemenda, 2009). Here we resume the results. It is assumed that the loss of a constitutive stability results in the initiation of a regular set of discrete (expressed not only in terms of the deformation rate, but also of the mechanical response) parallel compaction bands. The material within the bands undergoes inelastic loading/deformation, while outside the bands it is elastically unloading after initial elastic-plastic straining. The average spacing  $\lambda_0$  between the bands resulted from the bifurcation is

$$\lambda_0 = \frac{d_0 [18(h-h_{cr}^c)(2\nu-1)(\nu-1) + C_{\alpha\beta}]}{18(h-h_{cr}^c)(2\nu-1)(1-\nu)}, \quad (1)$$

where  $C_{\alpha\beta} = [2\beta(1+\nu) - 3N_3(2\nu-1)][2\alpha(1+\nu) - 3N_3(2\nu-1)]$ ,  $\alpha$  is the internal friction coefficient,  $\nu$  is the Poisson's ratio,  $h = H/G$  is the normalized hardening modulus,  $H$  is the hardening modulus,  $G$  is the shear elastic modulus,

$$h_{cr}^c = \frac{(1+\nu)(\beta-\alpha)^2}{9(1-\nu)} - \frac{1+\nu}{1-\nu} \left( \frac{1}{2}N_3 - \frac{\alpha+\beta}{3} \right)^2 - \left( 1 - \frac{3}{4}N_3^2 \right), \quad (2)$$

$h_{cr}^c$  is the normalized hardening modulus at which  $\lambda_0 = \infty$  or the spacing parameter  $\chi = d_0/\lambda_0$  is zero,  $N_3 = -0.5(N + 0.5\sqrt{4-3N^2})$ ,  $N = -s_2/\bar{\tau}$ ,  $s_2$  is the intermediate principal deviatoric stress,  $\bar{\tau} = (0.5s_{ij}s_{ij})^{1/2}$  is the Mises equivalent shear stress;  $\sigma_{ij}$  is the stress;  $s_{ij} = \sigma_{ij} - \delta_{ij}\sigma$  is the stress deviator,  $\delta_{ij}$  is the Kronecker delta,  $\sigma = \sigma_{ii}/3$  is the mean stress, the superscript “c” stands for compaction ( $i = 1, 2, 3$ ). The dilatancy factor  $\beta$  expresses the rate of change of the inelastic volumetric deformation  $\varepsilon^p$  with an inelastic equivalent shear deformation  $\bar{\gamma}^p$  and is defined as  $\beta = d\varepsilon^p / d\bar{\gamma}^p$  (Nikolaevskiy, 1967). Eq. (2) for  $h_{cr}^c = h_{\chi=0}^c$  is equivalent to that for the critical hardening modulus following from the continuous bifurcation analysis (Issen and Rudnicki, 2000; Ottosen and Runesson, 1991; Perrin and Leblond, 1993).

Download English Version:

<https://daneshyari.com/en/article/4693277>

Download Persian Version:

<https://daneshyari.com/article/4693277>

[Daneshyari.com](https://daneshyari.com)